

## The Performance and Remnant Life of Structural Steel in an Earthquake Damaged Building

W. G. Ferguson<sup>1</sup>, H. Nashid<sup>2</sup>, G.C. Clifton<sup>3</sup>, M V Kral<sup>4</sup>, S. Lopert<sup>5</sup> and G MacRae<sup>6</sup>

### Part A

### Abstract

The amount of inelastic (plastic) deformation sustained by an Eccentrically Braced Frame (EBF) in the steel framed, Pacific Tower (PT) building, following the Christchurch earthquake series of 2010/2011, is determined. A method for determining how much further plastic work damage can be absorbed without failure of the structural element is presented. Steel characteristics and the requirements of Steel Material Standards & Structural Steel Standards in building design and construction are reviewed. The measurement of plastic deformation in structural sections, following earthquake loading, is examined, possible methods reviewed and the hardness method outlined in detail. Correlation of hardness with plastic strain and flow stress is determined for a PT steel. Plastic strain distributions were measured in the web of as-received, undeformed, straightened structural steel beams as well as earthquake loaded, plastically deformed EBF active links. The results show there is a pre-existing plastic strain distribution resulting from roll straightening of the beam flange, which determines the locations for measuring hardness on the web, to estimate plastic strain generated by earthquake loading. The remnant plastic damage can thus be determined. The toughness of plastically deformed structural steel can be determined from previous research where toughness was determined, as a function of pre-strain for naturally strain-aged structural steel. Failure analysis of a fractured active link in an EBF system showed the fracture to be brittle and to have initiated at the site of a shear stud weld.

### Introduction

The Christchurch earthquake series of 2010/2011 generated intense shaking in the Central Business District, especially in the 22 February 2011 earthquake. Steel structures on the whole performed well during the earthquake series and the inelastic deformation was less than predicted, given the strength of the recorded ground accelerations. For steel buildings designed to withstand earthquake loading, a design philosophy is to have some structural elements deform plastically, absorbing energy in the process. In the most intense earthquakes in this series, some elements had significant plastic deformation and the buildings were structurally damaged. There is intense interest in how much further plastic work damage can be absorbed without failure of the structural element, as this determines whether damaged elements can be left in place or need replacing. This aspect is specifically examined in the Pacific Tower (PT) building, which is 22 storied, steel framed building with composite concrete floor on steel beams gravity system and Eccentrically Braced Framed (EBF) seismic resisting system.

### Structural Steel

It is just over 153 years since Bessemer set up the Bessemer Steel Company in Sheffield to make steel. Steel became more plentiful, less expensive and available for the railways, ship building and civil engineering infrastructure. Because of process control difficulties, the original process gave way to the Open Hearth process and eventually to the electric arc and oxygen processes in modern steel making. Most steel standards<sup>1</sup> do not allow "bottom blown processes to be used in the steel making method". In the late 1800's, Phosphorus (P) and Sulphur (S) were found to be detrimental to mechanical performance, especially under impact loading, in that they embrittled the steel and maximum limits had to be put on them to maintain ductility. By the early 1900's, Charpy and Izod impact tests were available to give some measure of toughness. Following WWII when arc welding became common, it was necessary to make structural steel readily weldable while still maintaining or increasing strength, ductility and toughness. Strengthening of structural steels is done with grain refinement, solid solution strengthening & precipitation hardening and an increase in toughness & decrease in transition temperature is achieved with grain size reduction. This has been achieved by:

<sup>1</sup>Professor Emeritus, Dept. of Chemical & Materials Engineering, University of Auckland, Auckland

<sup>2</sup>PhD Student, Dept. of Civil & Environmental Engineering, University of Auckland, Auckland

<sup>3</sup>Associate Professor, Dept. of Civil & Environmental Engineering, University of Auckland, Auckland

<sup>4</sup>Professor, Dept. of Mechanical Engineering, University of Canterbury, Christchurch

<sup>5</sup>BE (Hons) student, Dept. of Mechanical Engineering, University of Canterbury, Christchurch

<sup>6</sup>Associate Professor, Dept. of Civil & Natural Resources Engineering, University of Canterbury, Christchurch

- Reducing carbon content (lowers strength & transition temperature), generally limiting to no more than 0.25<sub>max</sub>% and raising manganese (Mn) content (raises strength & lowers transition temperature), with a maximum of 1.6%.
- To further lower the transition temperature, grain refining (reduction in ferrite grain size) has been introduced, which is achieved by aluminium (Al) treatment of the ladle, where aluminium nitride restricts grain growth. Grain refining elements include Al & titanium (Ti)<sup>2-9</sup>.
- Increased strength & lower transition temperature has been achieved by a reduction in carbon content & ferrite grain size. The latter is achieved by grain refinement using small/micro additions of vanadium (V) & niobium (Nb), which limit grain growth and also give precipitation hardening. Micro-alloying elements include Nb, V & Ti<sup>2-9</sup>.
- Higher strength and reduced transition temperature are obtained with a combination of Nb & V and Al treatments.
- Today the desired properties of structural steels are obtained by controlled rolling, also called thermo-mechanical processing, of micro-alloyed steels.

With highly restrained welds in thick plate, lamellar tearing can be a serious problem as experienced in New Zealand about 40 years ago, an example being the Reserve Bank of NZ, RBNZ, building in Wellington where highly constrained beam –column joints caused serious problems. Calcium (Ca) treatment, leading to much lower sulphur contents, less than 0.001%, and shape control of inclusions has alleviated this problem.

In using structural steel the engineer must be able to verify the steel meets specification. This is invariably done through the “heat number” or the Certificate of Analysis and Mechanical Test, which is essentially a ‘birth certificate’ and typically contains for structural steel: date, name of the steel works, steel making process, heat number, specification to which steel is made, section type (plate, column etc.), composition, mechanical properties, heat treatment, name of testing laboratory and name of organisation certifying laboratory. Today in New Zealand the testing laboratory must also have international accreditation as must all laboratories certifying structural steel for New Zealand use. The specification composition is that of the ladle analysis before casting, which today is generally a continuous casting process. The ladle analysis is the average composition of the steel in the heat. The composition of the ingots can be taken as the ladle composition, although the analysis of the ingot/product may vary from the specified ladle/cast analysis due to segregation arising during solidification. In steels, the element showing the greatest tendency to segregate is S, with P, C, Silicon (Si) and Mn segregating to a lesser extent and in that order. This means the composition in the ingot is non-uniform. Commercial steels also contain non-metallic inclusions, also called impurities, which mainly result from reactions taking place in the melt or solidifying metal and predominately include oxides and sulphides. If the properties of a structural steel are unknown the standards allow these, such as composition and mechanical properties, to be determined on the product following reasonably strict rules for sample selection etc.

**Table 1. Certificate of Analysis and Mechanical Test for AS/NZS 1163 C350 L0**

Orrcon Operations Pty. Ltd.  
Unanderra, NSW, Australia  
PH: +61 2 4271 4122  
FAX: +61 2 4271 3488  
Email: pipesales@orrcon.com.au  
ABN: 92 094 103 090





Page: 1 of 1  
Date: 13/09/11  
WO No.: 4545

**Test Certificate No.:** U4545 6246109 000217

**Product:** ERW 219.1 x 12.7 **Heat No:** 6246109

**Specification:** API 5L X42M PSL2 HFW, AS/NZS 1163 C350 L0, ASTM A53 B **Sample No:** 114545000217S

Chemical Analysis																				
Heat No.	Coil No.	Test	%C	%Mn	%P	%S	%Cr	%Nb	%Cu	%Mo	%Ni	%Si	%Ti	%V	%Al	%Sn	%B	CE (IW)	CE (Pcm)	Reference
6246109		L	.142	1.020	.012	.004	.015	.001	.016	.002	.012	.120	.002	<.003	.040	<.002		.31	.19	A28867
6246109	1H4H2258AB	P	.128	0.920	.011	.003	.014	.001	.020	.002	.015	.119	.006	.023	.041			.30	.18	ORRLAB/UN01/CN19
6246109	1H4H2258	P	.130	0.990	.018	.006	.029	.001	.020	.002	.013	.120	.002	<.003	.039	<.002		.30	.18	A28785

Mechanical Properties											
Heat No.	Coil No.	Test Freq	Test Sample	Heat Treatment	Yield Strength (MPa)	Tensile Strength (MPa)	%Elongation	%Elongation (L <sub>0</sub> =5.65S <sub>0</sub> )	Absorbed Energy (J)	Shear YS/TS Area % Ratio	Reference
6246109	1H4H2258AB	H	ChL	A					198	100	ORRLAB/UN01/CN19
6246109	1H4H2258AB	H	ChT	U					207	100	ORRLAB/UN01/CN19
6246109	1H4H2258AB	H&B	TP	U	421	491	40				ORRLAB/UN01/CN19 API 5L
6246109	1H4H2258AB	H&B	LT	A	440	500	28		28		ORRLAB/UN01/CN19 AS 1163

**Legend** L - Ladle Analysis; P - Product Analysis  
 CE Carbon Equivalent; If %C > 0.12  $CE(IW) = C + \frac{Mn}{6} + \frac{Cr + Mo + V}{5} + \frac{Ni + Cu}{15}$ ; If %C ≤ 0.12  $CE(Pcm) = C + \frac{Si}{30} + \frac{Mn + Cu + Cr}{20} + \frac{Ni}{60} + \frac{Mo}{15} + \frac{V}{10} + B$

This product has been manufactured under API License No. 5L-0464 using a quality system that complies with API Spec Q1, License Number Q1-0153, and ISO 9001, License Number ISO-0438. We certify that the material has been supplied in accordance with the product specifications listed on this test certificate. Inspections and tests covered include visual, ultrasonic (N10 Noth, dia 3.2 Hole), flattening, weld ductility, hydrostatic pressure (hoop stress of 90% of SMYS for 5 seconds), mass, dimensions and weld seam heat treatment (> 880 C). The test results reported on this certificate have been derived from tests performed by BlueScope Steel, and Orrcon Steel, both in accordance with the terms of NATA accreditation. NATA accreditation does not cover the performance of NDT and hydrostatic pressure testing.  
 Site Manager: John Croll

L0 - Gauge Length; S0 - Original Cross-sectional Area; H - Heat; B - Batch; A - Age; U - Ungaged  
 S - Strip; LT - Longitudinal Tensile; TW - Transverse Weld Tensile; TP - Transverse Pipe Tensile; RE - Ring Expansion  
 ChS - Strip Charpy Impact Test; ChT - Transverse Charpy Impact Test; ChL - Longitudinal Charpy Impact Test; ChW - Weld Line Charpy Impact Test; DWTT - Drop Weight Tear Test  
 Nominal Sample Dimensions (mm): S - 50.8 x 38.1; LT - 80 x 20; TW - 50.8 x 38.1; TP - 50.8 x 38.1; RE - 75; ChS - 10 x thickness; DWTT - 300 x 75; ChT, ChL & ChW - 10 x 10.0

The steel maker never makes each melt composition exactly the same; rather he/she keeps within the specification which allows for some variation for certain elements and maximum or minimum values for others, depending on the specification. To produce exactly the same composition each time would make the steel very expensive. Thus each melt is essentially unique, has a heat number and if necessary can be traced. The typical composition and properties for steel to AS/NZS 1163 C350 L0 is given Table 1, which is a Test Certificate (Certificate of Analysis and Mechanical Test) for such steel. This is an excellent example of such a certificate. The PT building was designed to NZS 3404:19972 incorporating Amendment No 1: 2001 and Amendment No 2:2007, however the S0 provision of the second amendment did not get put into the specification for the building<sup>10</sup>.

### Plastic Deformation of EBF Elements

Following the earthquakes, especially the 22 February 2011 event, some Eccentrically Braced Framed (EBF), active link webs were significantly plastically deformed and there was a need to determine the amount of plastic strain/damage that had been accumulated. This was required in order to determine whether they had sufficient residual life to still meet the New Zealand Earthquake Loading Code, NZS 1170.5 and be capable of sustaining a further severe earthquake. To this end, it was necessary to determine the plastic strain in the web section of the EBF. The available methods for determining plastic strain, are few, and include:

- Strain gauges & extensometers, which are inappropriate for they measure strain whilst it is being applied and not after its application and they rely on the strain being uniform.
- Comparison of deformed web with an un-deformed web using digital imaging; it would be possible to determine deformations and hence plastic strains, but a pattern would have to have been put on the web when the beam was made and the pre-earthquake geometry recorded in detail, which does not happen.
- Magnetic Barkhausen Noise<sup>11</sup>, MBN, which arises from the effects microstructure and plastic deformation etc. have on the magnetization curve, is not well developed as an established method.
- A method which has been used and which relies on a plastically deformed material getting harder when deformed, known as work hardening, is the hardness test. In this test, the material is deformed set amounts, the hardness measured and a correlation obtained of hardness versus either plastic strain or flow stress. The integrity of the method is dependent on the strength of the correlation between hardness and plastic strain which is dependent on how rapidly the material work-hardens with strain. Austenitic stainless steel work-hardens very rapidly and a strong correlation is obtained. With constructional steels, during the initial plastic straining, including the yield plateau, there is very little increase in strength and hence hardness. Following this region the increase in hardness will depend on the rate of work hardening up to the UTS. Also inherent in the technique is that there is always some scatter in hardness test results.

The usual and standard method of determining strength, such as yield stress,  $\sigma_y$ , and ultimate tensile strength, UTS,  $\sigma_u$ , is using the tensile test where yield stress, UTS, elongation to fracture and reduction in area can be determined with minimum error in an unambiguous way, such that the results have integrity. The hardness test is not a standard method for determining strength properties. The test is essentially used as a 'go-no-go' test to see if a material is within a particular specification band or a heat treatment is giving hardness in an acceptable range. For these reasons the test is acceptable, relatively easy to do and essentially non-destructive, provided fatigue is not a consideration. For determining flow stress and plastic strain, particular attention must be given to the experimental method. A method has been established and is in present day usage, especially in the Japanese Nuclear Industry<sup>11,12</sup>. These two papers by Nakane et.al.<sup>(11)</sup> & Matsumoto<sup>(12)</sup>, are of particular interest and are discussed below:

The paper by Nakane et.al.<sup>(11)</sup> refers to use of the technique in the Japanese Nuclear Industry and its particular use following the Niigata, Prefecture Earthquake in 2007, where the technique was used in assessing residual life in plastically deformed components at a reactor site. They used various portable hardness testers to determine hardness versus plastic pre-strain and also investigated the effect of cyclic plastic pre-strain, up to  $\pm 8\%$  plastic strain, on strength and fatigue life. For the steels they used, they concluded 2% pre-strain was the detection limit for the hardness measurement technique. They suggested "that the estimation of plastic strain from the materials hardness is sufficiently accurate for assessing the remaining fatigue life of the components in nuclear power plants".

Matsumoto<sup>(12)</sup>, concluded that, for uniform elongation, there was a clear correlation of hardness with elongation. The hardness was measured with a portable Leeb hardness tester. He also concluded that the hardness technique was a useful method for estimating the residual deformation capacity of steel after a

severe earthquake. Uniform and cyclic deformation, were used for pre-straining. The effect of cyclic pre-straining is not clear and the correlation of yield stress against hardness for such pre-straining shows a large amount of scatter. Matsumoto also noted that the yield stress for monotonic loading tended to be higher than for cyclic loading.

Clearly, the hardness technique can be used to determine plastic deformation in steel using portable hardness testers. It is not clear what the accuracy of the process is and also cyclic plastic pre-strain would appear to be important in determining the correlation. Once the plastic strain in the web has been determined, the residual life can be determined for it will be a function of the strain at the UTS; if loaded to the UTS strain, there would be no residual life, fracture being the next deformation event. If the UTS plastic strain was 15% and the web plastic strain from EQ plastic deformation 7.5%, then the residual life would be 50%.

### Hardness Technique

The research discussed below has been undertaken by Hassan Nashid, a PhD research student in the Department of Civil & Environmental Engineering, at the University of Auckland. The experimental work and method are detailed in a paper to be presented to the 2013NZSEE Conference<sup>14</sup>. To commence the investigation into using hardness as method for determining plastic strain in deformed structural steel, tensile specimens made from Grade 300MPa steel, were loaded to various plastic strains as shown in Figure 1.

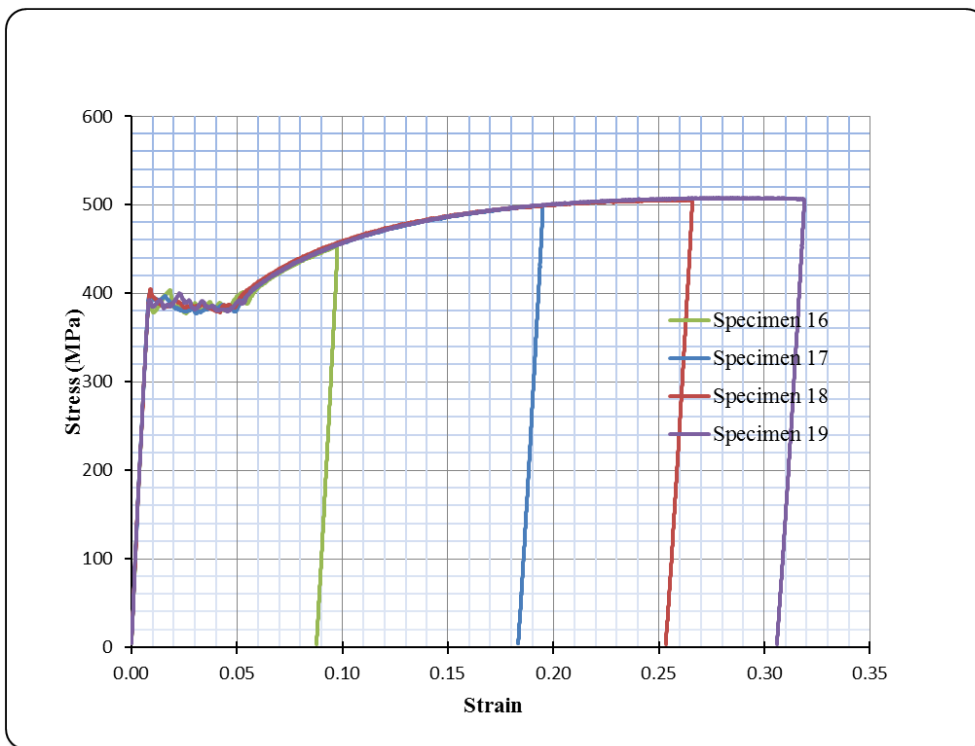


**Figure 1** Stress – Strain curves for tensile specimens S16, S17, S18 and S19

After deformation the Rockwell B hardness was measured on each specimen numerous times and the results are plotted in Figure 2, where Rockwell B hardness is plotted against percentage plastic strain. This figure then is a correlation of hardness with plastic strain and can be used to determine plastic strain in a similar steel that has been plastically strained. The inherent errors in the process can be noted from the range of Rockwell B data at each strain. This correlation should not be used with the data from the remainder of the paper because the steels are not the same. Another way to make the correlation is to plot flow stress against hardness and from such a curve determine flow stress and relate this to plastic strain from the stress-strain curve for the steel. This method does not reduce the inherent errors in the hardness method.

Hardness and tensile tests were conducted on the web of an EBF system which had been plastically deformed during the 22<sup>nd</sup> February 2011, earthquake and removed from level 3 of the Pacific Tower. The EBF system was divided into three test zones as shown in Figure 3(a): Active Link Zone (Zone-A), Panel Zone (Zone-B) and Beam Zone (Zone-C), and the tests were conducted on the web section of each zone. Three tensile specimens were, water jet cut, from each zone as indicated in Figure 3(a) and hardness tests taken in a grid pattern as indicated in Figure 3(b) where there were 25 test locations and at least 6 tests were

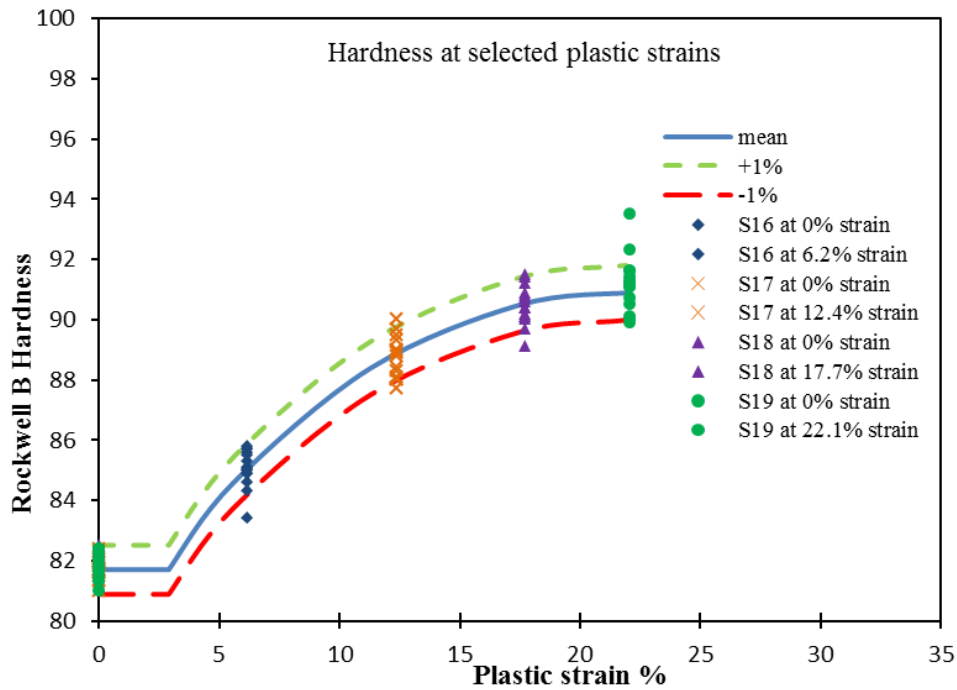


**Figure 2** Hardness versus Plastic Strain relationship for 8mm thick tensile specimens

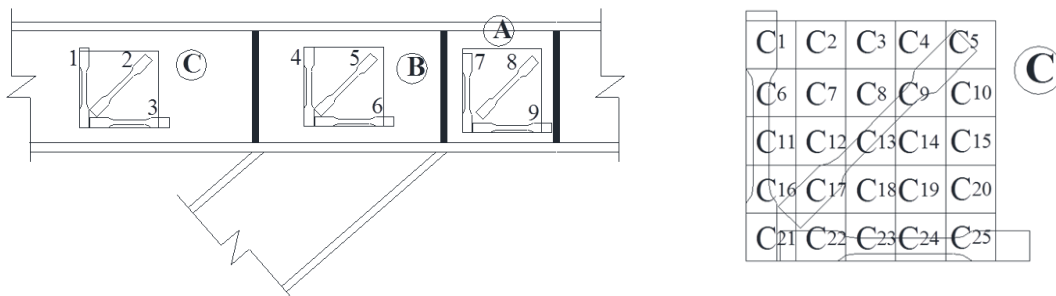


**Figure 3(a)** Tensile specimen locations in zones A, B & C of the active link beam **Figure 3(b)** Hardness test grid for zone C (Similar for zones A & B)

done at each location. Both Rockwell B and Leeb, model TH170, hardness testers were used<sup>14</sup>. The Leeb TH170 is a portable hardness tester<sup>15</sup>, which enables on site testing, but requires careful surface preparation with the surface roughness being less than  $1.6 \mu\text{m}$  and the test specimen needs a minimum weight<sup>14</sup> of 5 Kg.

The Leeb hardness, which can be read as a Rockwell B hardness, for each of the grids in zones A, B & C is plotted in Figure 4, as hardness Rockwell B versus grid number. It can be seen the hardness in zone A, the active link, is within the scatter, constant and higher than for the other zones. This is the zone that would be plastically deformed. For the other zones it can be seen the hardness is significantly lower in the middle rows of the grid, corresponding to the central portion of the web, where for these zones there should no plastic deformation. For the edge rows near the flanges the hardness has increased significantly to about the level for zone A, which implies there has been plastic deformation in this region next to the flanges in these zones. To examine this effect further the hardness data for both Rockwell and Leeb testers are plotted in Figure 5 as normalised link/beam depth versus Rockwell B hardness for one column of data from each of the zones A, B & C. Firstly the Rockwell B test results are about 10 points higher than for the Leeb, but both show the same trends, in that for the zone deformed by the earthquake, the hardness is essentially constant across the web between the flanges and for zones B & C there is no plastic strain in the centre of the web but there is some near the flanges and of the same magnitude as that in zone A. If the tensile stress-strain

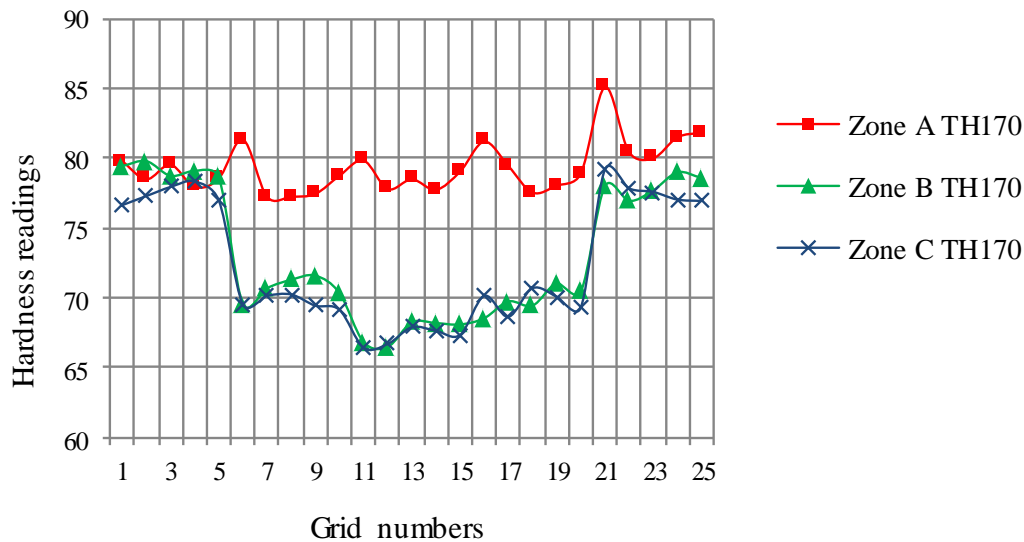


**Figure 4** Rockwell B hardness versus grid numbers in zones A, B & C of the active link beam from level 3, Pacific Tower (Leeb hardness tester)

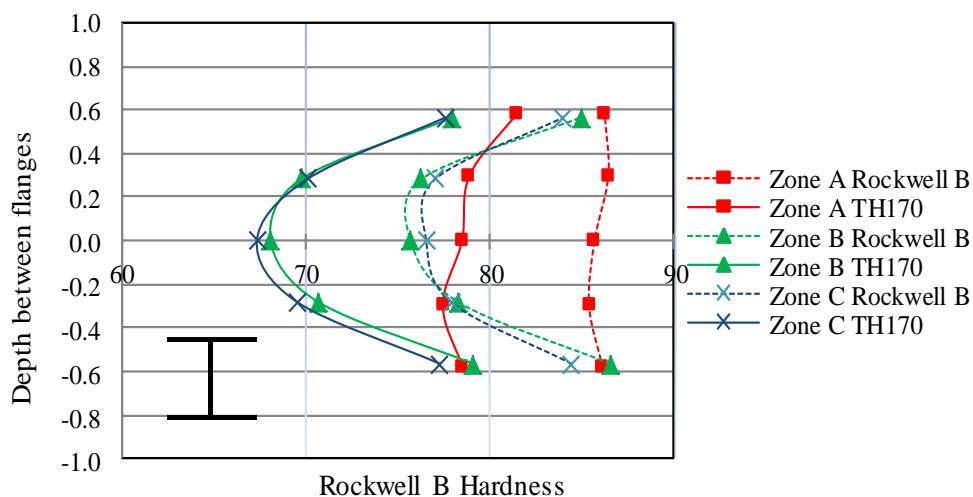


**Figure 5** Rockwell B hardness versus normalised link depth between flanges for the zones A, B & C of the active link beam from level 3, Pacific Tower ( Leeb & Rockwell hardness testers)

curves in Figure 6, for each of the tests in zones A, B & C are examined, it can be seen that they confirm the hardness results. All tests from zone A, 7, 8 & 9, have essentially the same shaped cure and flow stress which is to be expected as this web should have been deformed plastically in the earthquake. For zones B & C, tests 1, 4, 2 & 5, have essentially the same shaped yield curve and yield stress, which is to be expected as the centres of these specimens are in the centre of the web which for these zones should not have yielded. Tests 3 & 6 are near the flange, have the same shaped stress-strain curve, but the flow stress has increased over that for tests 1, 4, 2 & 5, showing there has been plastic deformation in the region of the web near the flange and confirming the hardness results. Clearly from these results, the as received beam has been plastically deformed near the flanges. The curves also show that this manufacturing plastic strain is about 3% and the plastic strain in the deformed zone A is about 7 – 7.5%.

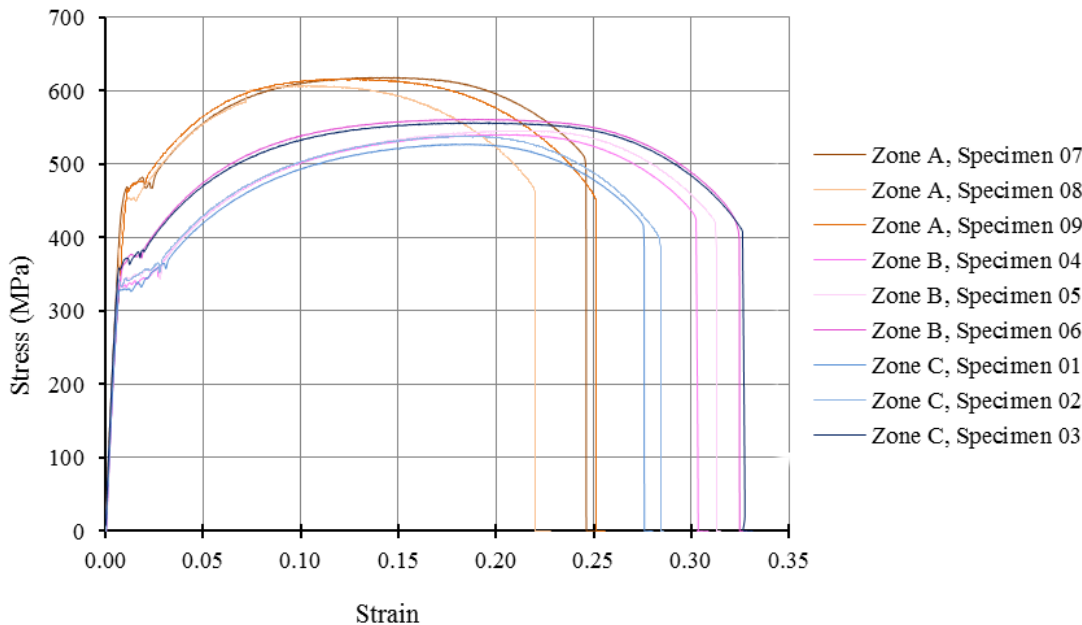


**Figure 6** Stress – Strain curves for tensile specimens from zones A, B & C of the active link beam from level 3, Pacific Tower

Several photographs of deformed links, one of which is shown in Figure 7, from damaged buildings in Christchurch, show the paint has peeled from the central portion of the web but near the flanges the paint is still adhering to the steel indicating it has not been plastically deformed. The initial concern was that the flanges were affecting the Leeb hardness but when the flanges were cut off and Rockwell B measurements taken the effect was still present which was confirmed by the tensile tests. A literature search showed the



plastic strain in a 'virgin' beam to arise from roll straightening at temperatures below 100°C. Tide<sup>16</sup> sectioned an as received beam and did a Rockwell B hardness traverse across the cross-section near the web and flange and reported the same behaviour, with plastic deformation of the web near the flanges caused by final cold straightening of the beam flanges in manufacturing the beam. The implications of the findings, are that hardness testing to check for plastic deformation, has to be done in the centre of the web and similarly tensile specimens have to be taken in the centre of the web and parallel to the flange.

**Figure 7** An Active Link beam at the Club Tower

To-date there has been no correlation made of hardness with plastic strain for the PT steel, as that work is yet to be done.

### Structural Steel Toughness

To simulate the effect of fabrication and earthquake loading, plastic strains, the Charpy V-Notch, CVN, impact energy toughness of steel tensile specimens taken from the flanges of a 310UC158 column section, compatible with Hot Rolled Steel Sections Standard, AS/NZS 3679.<sup>3,5</sup>, were pre-strained in monotonic tension to 4.9%, 9.8% and 17.7% engineering strain, then aged naturally and the Charpy V-Notch energy, determined at various temperatures<sup>17</sup>. The results are shown in Figure 8, where CVN is plotted as a function of test temperature. Pre-strain raises the transition temperature curve, increasing with increasing pre-strain. To ensure steels used in seismic resisting structures maintain ductility demand, the New Zealand Steel Structures Standard NZS 3404 Amendment No 2:2007 and Hot Rolled Sections manufacturing standard AS/NZS 3679.1, have been changed to ensure constructional steels for seismic application have a minimum CVN energy of 70 J @ 0°C.

From Figure 8, the shift in the transition temperature of deformed, strain-aged steel for a plastic strain of 4.9% raises the transition temperature by about 20°C, but the steel would still meet the toughness

requirement of 70 J at 0°C. set by Standard, NZS 3404. Within the scatter it might be argued that the upper limit for the peak plastic strain, resulting from earthquake loading and still ensuring the that70 J at 0°C requirement is met, is about 7.5%, and the link examined above would meet the requirements of the standard.

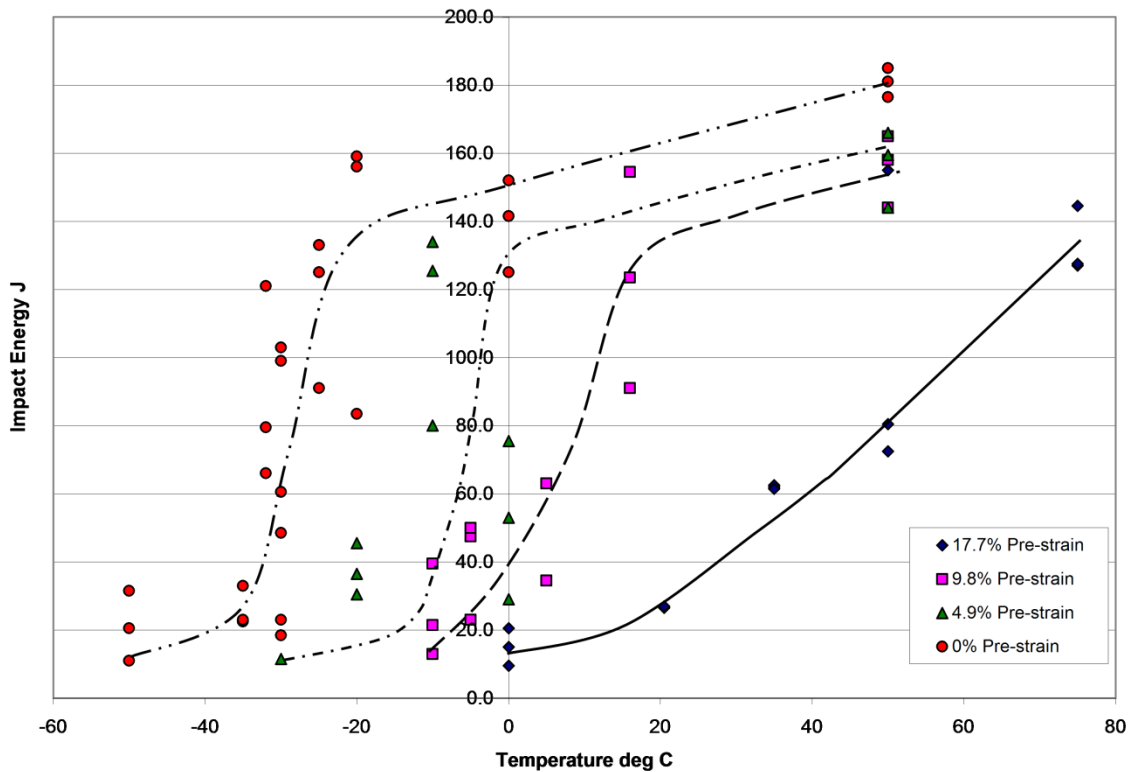


**Figure 8** Charpy V-Notch transition curves showing effect of pre-strain<sup>17,18</sup>

### Failure Analysis

Failure analysis of a fractured active link in an EBF on level 6, is presented in Section B.

### Conclusions

- A working understanding of the materials aspects of the standards, the steel mill certificate and the implications of the testing authorities is essential for today.
- In spite of concerns over the hardness technique for determining plastic strain, it is however the only method available which has some credible previous use, namely the Japanese Nuclear Industry, that is available to determine the non-uniform plastic strain in steel.
- The portable Leeb hardness tester appears to give consistent results when compared with the Rockwell B method
- When using a correlation of plastic strain with hardness it is important to understand the variation/scatter with hardness results.
- The hardness variations in the EBF link beam were confirmed by tensile tests.
- When doing hardness tests to confirm plastic deformation arising from earthquake loading, the testing must be done in the centre of the beam web. Similarly tensile specimens should be cut parallel to the flanges in the centre of the web.
- There was about 7 – 7.5% plastic strain in the active link beam.
- In the panel and beam zones there was pre-existing plastic strain near the flanges produced by the manufacturing process where there is low temperature roll straightening of the flanges. This strain was about 3%.
- The plastically deformed steel would still just meet the 70 J at 0°C Charpy impact energy toughness requirement.

- It must be noted that following plastic straining, the structural engineer is not commencing with virgin hot rolled structural steel of known properties as specified in some standard. Following plastic deformation, the composition will be unaltered, the strength slightly increased but the steel will have strain-aged and the elongation/ductility/toughness will have decreased and the capacity for further plastic deformation, reduced. How much remnant life is required with such a material, is not a trivial question and is a structural engineering problem.

### References

1. NZS/BS 970.1:1991 Wrought steels for mechanical and allied engineering purposes
2. NZS 3404:Part1:1997 Steel Structures Standard
3. AS/NZS 3679.1:1996 Structural Steel Part 1: Hot-rolled bars and sections
4. AS/NZS 3679.2:1996 Structural Steel Part 2: Welded I sections
5. AS/NZS 3679.1:2010 Structural Steel Part 1: Hot-rolled bars and sections
6. AS/NZS 3678:1996 Structural Steel – Hot-rolled plates, floorplates and slabs
7. AS/NZS 3678:2011 Structural Steel – Hot-rolled plates, floorplates and slabs
8. AS/NZS 1594:2002 Hot-rolled steel flat products
9. AS/NZS 1163:2009 Cold-formed structural steel hollow sections
10. Associate Professor G. Charles Clifton, Private Communication, 2013
11. Stewart, D. M., K. J. Stevens and A. B. Kaiser, 2004, Magnetic Barkhausen noise analysis of stress in steel, *Current Applied Physics*, Vol. 4, Issues 2-4, 308 - 311
12. Accuracy of Plastic Strain Estimated by Hardness to Assess Remaining Fatigue Lives, M. Nakane, Hitachi, Ltd., Japan; S. Kanno, Hitachi-GE Nuclear Energy, Ltd., Japan; Y. Kurosaki, Y. Takagi, Tokyo Electric Power Company, Japan; J. Komotori, Keio University, Japan; T. Ogawa, Aoyama Gakuin University, Japan, *Material Properties Measurement*
13. Study on the residual deformation capacity of plastically strained steel, Yuka Matsumoto, Yokohama National University, Yokohama, Kanagawa, Japan, 2009 Taylor & Francis Group, London, UK
14. Nashid, H., W. G. Ferguson, G. C. Clifton, M. Hodgson & C. Seal, 2013, Non-destructive hardness testing method to investigate the amount of plastic strain in cyclically deformed structural steel elements – Christchurch earthquake series 2010/2011, 2013, 2013NZSEE Conference
15. ASTM A956-06 Standard Test Method for Leeb Hardness Testing of Steel Products
16. Tide, R. H. R., 2000, Evaluation of steel properties and cracking in “k”-area of W shapes, *Engineering Structures*, 22, 128 - 134
17. PhD Thesis: Clark W K Hyland, The University of Auckland, 2008
18. Hyland, C. W. K., W.G Ferguson and J.W. Butterworth, Selection of Structural Steel for Seismic Performance, 2<sup>nd</sup> New Zealand Metals Industry Conference, N.Z. HERA, Nov., 2004.

### Part B

# Failure Analysis of the Active Link in an Eccentrically Braced Frame

Milo V. Kral<sup>1</sup>, Samuel Lopert<sup>1</sup> and Charles Clifton<sup>2</sup>

<sup>1</sup>University of Canterbury, Department of Mechanical Engineering

<sup>2</sup> University of Auckland, Department of Civil and Environmental Engineering

## I. Introduction and Background

The 6.3 magnitude earthquake that struck Christchurch on the 22nd of February 2011, caused widespread damage to many structures in the city, especially the 6 buildings of around 20 storeys in the central business district. This was due to the very high intensity of this earthquake, with the highest peak ground accelerations recorded worldwide in a first world city. The 22-storey Pacific Tower, located on Gloucester St, was no exception. The eccentrically braced frames that comprise the seismic resisting systems underwent inelastic action in their active links. In July 2011, workers discovered that one of the active links in an EBF located in the Northwest corner of the tower had fractured (see Figure 1). This type of EBF fracture had not been reported worldwide in either laboratory testing or other earthquakes. The fractured link was cut out of the building and investigated further.

Eccentrically braced frames (EBF's) are a lateral load resisting system for steel buildings that are well suited to high seismic regions due to their high stiffness, favorable ductility and high capacity for energy-dissipation. The subject of the present investigation was a K-type EBF. EBF's are designed to ensure that any inelastic activity is concentrated into the active links, and that buckling failures in either the braces or the columns are prevented. Designing the active links to yield in a severe earthquake effectively limits the maximum force that is transferred into the braces, collector beams and columns and limits damage to other components of the structure.

## II. Fractography and Metallography

The fractured active link was removed from the building and sectioned to reveal the fracture surfaces. Examination of the fracture surfaces revealed that the initiation site was at a shear stud weld (Figure 2). Headed shear studs were welded the surface of the upper flange of the active link during construction and embedded into the concrete slab, with their role to generate composite action between these two components. Shear studs are welded within a ceramic ferrule and use the base of the shear connector itself as the weld metal. During welding they shorten by 5 - 7mm as the base of the stud and the supporting steel beam directly underneath are melted and fused together. Metallographic examination and hardness traverses of the welded zone (see Figure 2) revealed that there were slag inclusions and untempered martensite in the microstructure. Note that shear studs were located at the corners of the active link (see Figure 1), just above the stiffening plates, a location that would have needed to yield under high demands for strain in the event of lateral loads.

Visual examination suggested that the upper flange and web of the active link fractured in a brittle manner, due the absence of any signs of plastic deformation (such as shear lips) and presence of chevron marks. Chevron marks showed that the fracture propagated from the weld material through the upper flange, through the web, and arrested at least three times in the lower flange (see Figure 3). It is possible that the arrests correspond to three different seismic events. It cannot be ruled out that there was a large crack pre-existing the first earthquake on 4 September 2010, or the much more intense 22 February 2011 earthquake, since there was heavy corrosion and concrete on the fracture surface at the initiation site,

while the fracture surface through the web was relatively clean and free of corrosion. Scanning electron fractography (Figure 4) showed that the entire fracture surface was dominated by cleavage, which can only be interpreted as impact loading at a temperature below the ductile brittle transition temperature (DBTT).

### III. Charpy Tests and Analysis

To further characterize the material's performance, a series of Charpy impact tests were performed over a range of temperatures from -70°C to 100°C. There are several possible choices to model Charpy Impact Energy vs. temperature. We used the hyperbolic tangent model:

$$C_i = a + b \tanh ((T_i - T_0)/C^*)$$

where:

$a + b$  = the upper shelf temperature (use the maximum energy obtained)

$a - b$  = the lower shelf temperature (use the lowest energy obtained)

$T_i$  = the temperature of interest

$T_0$  = the midpoint between the upper and lower shelf temperatures

$m$  = the slope at the midpoint

$C^* = b/m$

$C_i$  = the energy at the temperature of interest

If one defines the ductile brittle transition temperature (DBTT) as the temperature as the impact energy passes through 27J, then the hyperbolic tangent model fitted to the experimental data (see Figure 5) identifies the DBTT of this material as 11.5°C. The impact energy at 0°C (relevant to grade 300L0) is only approximately 12J.

### IV. Conclusions

The failure of the active link in the EBF was a consequence of at least three factors:

1. the unfortunate location of the shear studs;
2. the low impact fracture energy of the material at ambient temperatures;
3. the impact loading due to seismic activity.



*Figure 1: Fractured EBF in situ.*

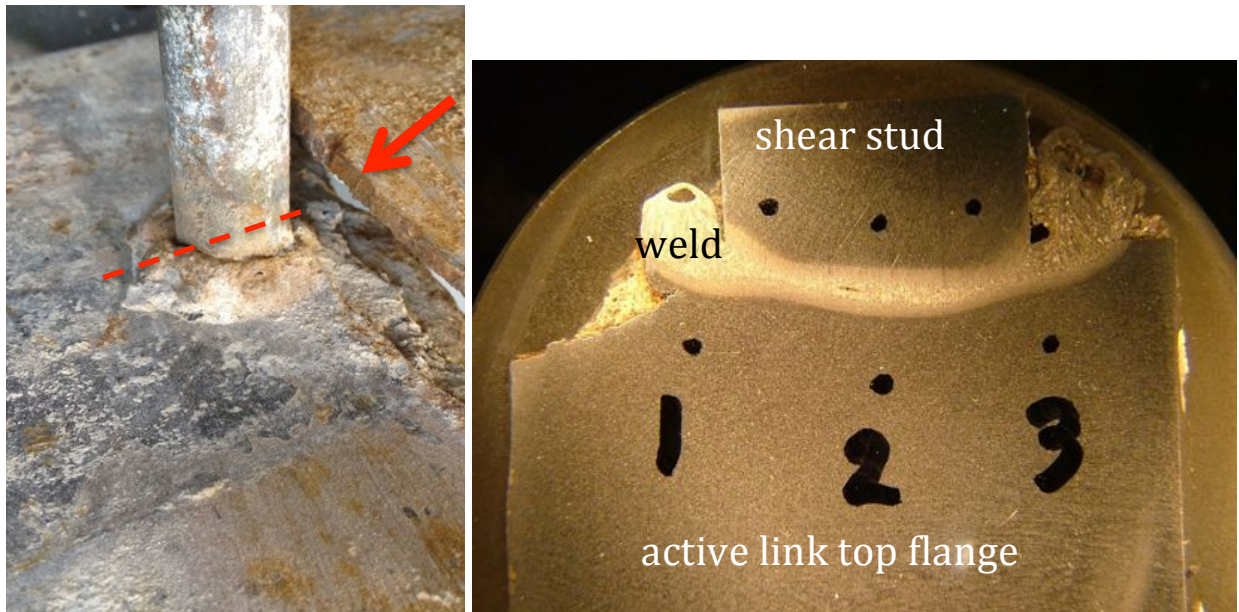


*Figure 2 - The red arrow indicates the initiation site is near the toe of the weld (left image). The red dashed line indicates where the shear stud was cross sectioned. Metallography and microhardness traverses through the weld of the shear stud (right image) indicate the presence of non-metallic inclusions and untempered martensite.*



*Figure 3: One of the fracture surfaces. The red arrow indicates the initiation site. The white arrows show arrest marks.*

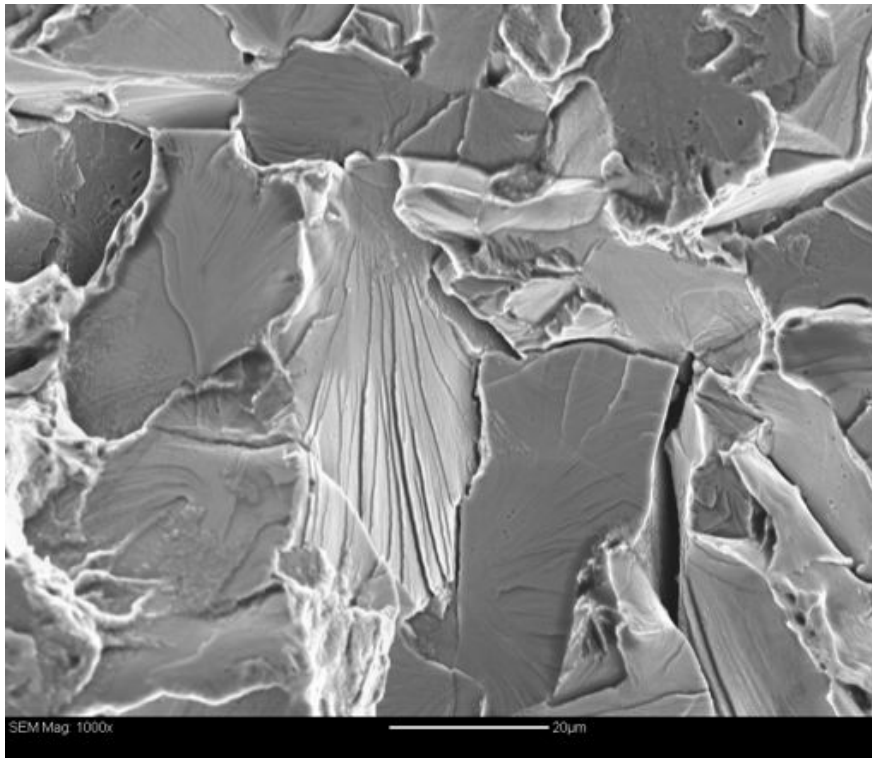


Figure 4: Scanning electron micrograph showing the typical appearance of the fracture surface. The appearance is classic cleavage fracture of steel subject to impact loading below the ductile-brittle transition temperature.

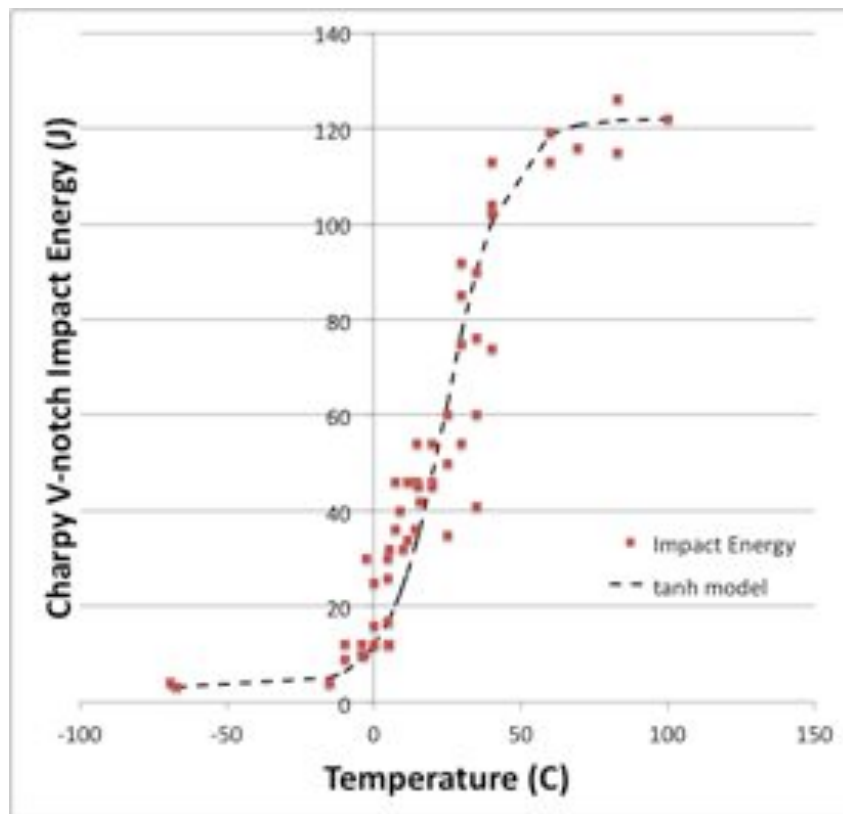


Figure 5 - Charpy V-notch energy versus temperature data with hyperbolic tangent function fit.